

# NEUTRINO INDUCED REACTIONS ON NUCLEI IN THE LAB AND IN STARS\*

EDWIN KOLBE

Departement für Physik und Astronomie der Universität Basel  
Klingelbergstrasse 82, CH-4056 Basel, Switzerland

*(Received May 8, 2000)*

The important role of neutrino induced reactions on nuclei at low and intermediate energies both in accelerator-based experiments in Neutrino Physics and in Neutrino Astrophysics is discussed. After a short description of the theoretical nuclear model we present selected applications to various neutrino experiments. We will focus on the sensitivity of neutral current neutrino scattering to the strangeness content of the nucleon and on the calculation of neutrino induced reactions on  $^{56}\text{Fe}$  and  $^{208}\text{Pb}$ , which have been discussed as target materials in future neutrino detectors.

PACS numbers: 25.30.Pt, 13.15.+g

## 1. Introduction

Neutrinos play a decisive role in many aspects of astrophysics and determining their properties is considered the most promising gateway to novel physics beyond the standard model of elementary particle physics. Thus detecting and studying accelerator-made or astrophysical neutrinos is a forefront research issue worldwide with many ongoing and planned activities.

One of the fundamental questions currently investigated is whether neutrinos have a finite mass. This question can be answered by the potential detection of neutrino oscillations which would establish the existence of at least one family of massive neutrinos. Furthermore, the existence of massive neutrinos might have profound consequences on many branches of cosmology and astrophysics, *e.g.* the expansion of the universe and the formation of galaxies, while neutrino oscillations can have interesting effects on supernova nucleosynthesis [1].

---

\* Presented at the Cracow Epiphany Conference on Neutrinos in Physics and Astrophysics, Cracow, Poland, January 6–9, 2000.

From the many experiments directly searching for neutrino oscillations, only the LSND collaboration has reported positive candidate events [2]. Indirect evidence for neutrino oscillations arises from the deficit of solar neutrinos, as observed by all solar-neutrino detectors [3], and the suppression and its angular dependence of events induced by atmospheric  $\nu_\mu$  neutrinos in SuperKamiokande [4, 5]. Due to the obvious importance, the oscillation results implied from these experiments will be cross-checked by future long-baseline experiments like MINOS [6]. From the detectors currently operable KARMEN [7] has a neutrino-oscillation sensitivity similar to the LSND experiment. Currently, the KARMEN collaboration does not observe oscillations covering most of the oscillation parameter space for the positive LSND result [8].

It is the aim of this article to point out the role that neutrino induced reactions on nuclei play in the field of Neutrino Physics and Neutrino Astrophysics. In the next section we firstly describe the theoretical models that we use to calculate semileptonic weak interactions in nuclei. In the third part we present four applications of the theory to various neutrino experiments. Finally Section 4 is given over to conclusions.

## 2. Theory

### 2.1. Continuum random phase approximation (RPA)

A schematic plot of a cross section characteristic for medium energy neutrino scattering on nuclei is shown in Fig. 1. We assume that the incoming neutrino has a medium energy of  $E_\nu \approx 50$  MeV and plot the cross section as

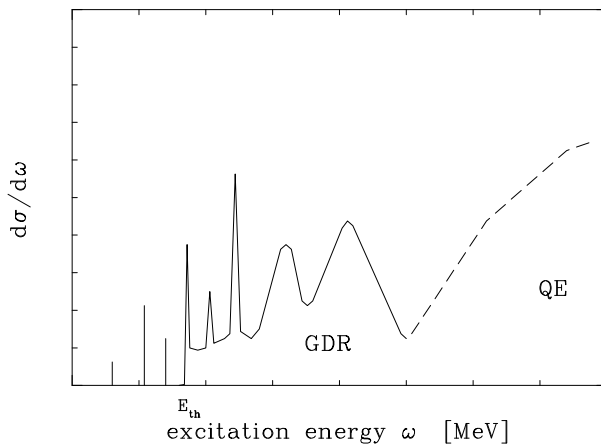


Fig. 1. Schematic plot of a typical cross section for medium energy neutrino scattering on an iso-scalar nucleus.

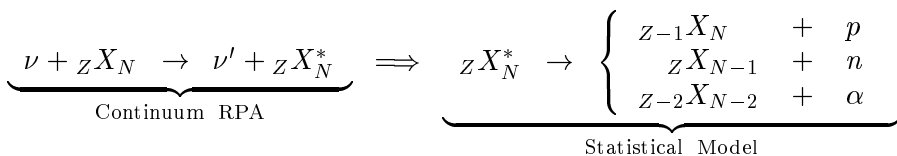
a function of the excitation energy  $\omega$  in an iso-scalar target nucleus ( $T_i = 0$ ). As neutrinos dominantly induce iso-vector transitions ( $\Delta T = 1$ ), it is found that the lowest lying states that get remarkable strength are (if present at all) a few discrete states with isospin  $T_f = 1$ . Next, above particle emission threshold ( $E_{th}$ ), small iso-vector resonances show up and collect some strength. However, the dominant contributions to the total cross section come from the broad states in the giant dipole resonance (GDR) region, which are known to have the structure of collective one-particle-one-hole ( $1p-1h$ ) excitations. At last, very energetic neutrinos may scatter quasi-elastically (QE) and knockout (single) nucleons from the nucleus.

These final nuclear states dominantly excited in neutrino scattering are nicely described by the continuum RPA model. As the model has been dealt with in detail in Ref. [9], it is appropriate that we just briefly outline its features in the following. In this approach the usual RPA treatment is combined with a correct description of the particle states in the continuum, *i.e.*, the excited many-body states are coherent superpositions of one-particle-one-hole ( $1p-1h$ ) excitations obeying the proper Coulomb boundary conditions for scattering states. Its basic properties can be summarized by:

1. the nuclear ground state is well described,
2. the excited states are generic continuum states of  $1p-1h$  structure,
3. final state interactions are accounted for with a realistic (finite range) residual interaction derived from the Bonn meson exchange potential [10, 11],
4. this model has been shown [9, 12] to yield a good description of the giant (dipole and spin-dipole) resonances in light nuclei, *e.g.*, in  $^{12}\text{C}$  and  $^{16}\text{O}$ ,
5. especially charge exchange reactions of the knocked out nucleon are included in the model.

### 2.2. Statistical model

To calculate cross sections for  $X(\nu, \nu'x)Y$  and  $X(\nu_l, l^-x)Y$  reactions, *i.e.*, for the neutrino induced knockout of a particle, we assume a two-step process (here shown for neutral current scattering):



In the first step the cross section for neutrino excitation is determined within the continuum RPA model. In the second step we calculate for each final state with well-defined energy, angular momentum and parity the branching ratios into the various decay channels using the statistical model code SMOKER [13], considering proton, neutron,  $\alpha$  and  $\gamma$  emission. As possible final states in the residual nucleus the SMOKER code considers the experimentally known levels supplemented at higher energies by an appropriate level density formula [13]. Note that the SMOKER code has been successfully applied to many astrophysical problems and that we empirically found good agreement between  $p/n$  branching-ratios calculated with SMOKER and within continuum RPA for several neutral current reactions on light nuclei [14].

### 2.3. Global approach

In the demanding field of theoretical nuclear physics (several body system with strong interaction) it is especially necessary to test a nuclear model before applying it to any problem. The continuum RPA has the advantage that it can be used to describe a wide range of weak as well as electromagnetic interactions in nuclei (global approach). Therefore we could test it against various available data:

- The calculated longitudinal and transverse response for electron scattering on  $^{12}\text{C}$  is in good agreement with the experimental data [15].
- We described all neutrino induced reactions  $^{12}\text{C}$  measured by the KARMEN-group [7] and find good agreement between our theoretical results and the data [16].
- Especially total muon capture rates are reproduced very well within continuum RPA [17]. Note, that to describe neutrino scattering and muon capture rates the same nuclear matrix elements must be calculated.

## 3. A selection of applications

### 3.1. Supernova neutrino signal

Nearly all the energy of a Type II supernova is released by (anti)neutrinos of all flavors, which are mainly generated with equal luminosity by  $e^- + e^+ \leftrightarrow \nu + \bar{\nu}$  reactions. But, as  $\nu_\mu$  and  $\nu_\tau$  neutrinos and their antiparticles (in the following denoted by  $\nu_x$ ) have lower opacities, they decouple at smaller radii and therefore have higher energies than  $\nu_e$  and  $\bar{\nu}_e$  (anti)neutrinos.

Model calculations of supernova explosions give average neutrino energies of  $\langle E_{\nu_x} \rangle = 25$  MeV for  $x = \mu, \tau$  (anti)neutrinos, and  $\langle E_{\bar{\nu}_e} \rangle = 16$  MeV,  $\langle E_{\nu_e} \rangle = 11$  MeV.

In water Čerenkov detectors neutral current scattering reactions on  $^{16}\text{O}$  induced by the higher energetic  $\nu_x$  neutrinos can be used to uniquely identify supernova  $\nu_\mu$  and  $\nu_\tau$  neutrinos. The detection scheme is illustrated in Fig. 2, and based on the following facts: (i) The new SuperKamiokande (SK) de-

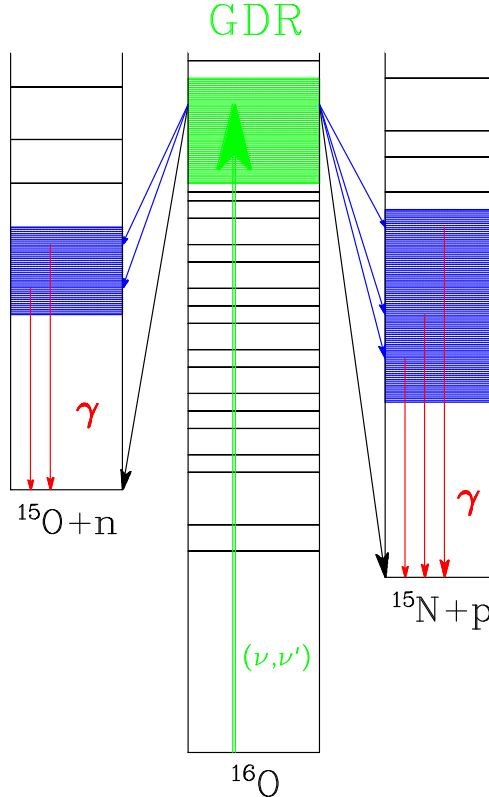


Fig. 2. Schematic illustration of the detection scheme for supernova  $\nu_\mu$ - and  $\nu_\tau$ -neutrinos in water Čerenkov detectors.

tector has a lower threshold of  $E_{\text{th}} = 5$  MeV [18], (ii) The daughter nuclei  $^{15}\text{N}$  and  $^{15}\text{O}$ , that are left over after neutrino-induced knockout of a nucleon on  $^{16}\text{O}$ , have both first excited states with energies larger than 5 MeV ( $E^* = 5.27$  MeV in  $^{15}\text{N}$  and  $E^* = 5.18$  MeV in  $^{15}\text{O}$  [19]), (iii) as  $\nu_e$  and  $\bar{\nu}_e$  have lower energies, they do not significantly contribute to the signal shown in Fig. 2. Within the theoretical model described in Section 2 we calculated in detail the cross sections for neutrino excitation of  $^{16}\text{O}$  levels and the subsequent branching ratios into the various decay-channels [20]. It was found

that by  $^{16}\text{O}(\nu_x, \nu'_x)$ -reactions mainly  $1^-$  and  $2^-$  states in the giant resonance region are excited and dominantly decay by proton and neutron emission. Furthermore a significant fraction of these decays,  $\approx 24\%$  for  $^{15}\text{N}$  and  $\approx 6\%$  for  $^{15}\text{O}$ , do not end in the ground state of the daughter nucleus, but go to excited states, which decay by photon emission. Taking into account the neutrino flux from a supernova at 10 kpc (*i.e.* within our Galaxy) and the number of target nuclei in SK it turned out that in the energy window  $E = 5\text{--}10$  MeV the yield of photons from  $(\nu, \nu' p \gamma)$ - and  $(\nu, \nu' n \gamma)$ -reactions on  $^{16}\text{O}$  is noticeably larger than the positron or electron background expected from other neutrino reactions in water (This is demonstrated in Fig. 2 of Ref. [20].) Therefore  $(\nu, \nu' N \gamma)$ -reactions on  $^{16}\text{O}$  constitute a unique signal for supernova  $\nu_\mu$  and  $\nu_\tau$  neutrinos in water Čerenkov detectors.

### 3.2. Strange quark contributions to neutral current neutrino scattering

Experiments [21,22] have suggested that in addition to the valence quarks in the nucleon also pairs of  $s\bar{s}$ -quarks contribute to nucleonic properties like, *e.g.*, the proton-spin. (For a more extended discussion of this topic we refer to Refs. [23,24].) If present, this  $s\bar{s}$ -sea or strangeness in the nucleon will also affect neutral current neutrino scattering on nuclei, because the  $Z^0$ -bosons mediating these processes can couple to all quarks inside the protons and neutrons of the nucleus. This is illustrated in Fig. 3.

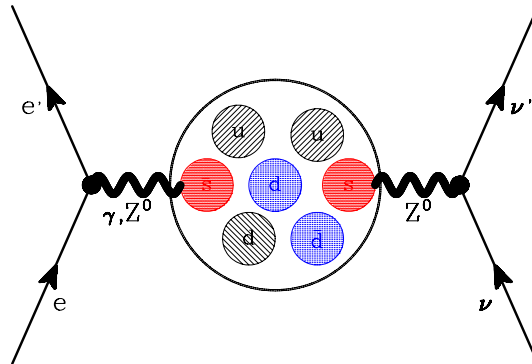


Fig. 3. Leptonic interactions with the proton

For another more technical explanation of the connection between  $s\bar{s}$ -sea in the nucleon and neutral current neutrino scattering we remind ourselves that neutrino scattering cross sections are accurately obtained within first order Born approximation and that the weak Hamiltonian can be written, according to the Standard Model, in current-current form. Thereby leptonic

and hadronic currents have the well-known (V – A)-structure:

$$j_{\lambda}^{(0)} = \bar{\psi}_{\nu} \gamma_{\lambda} (1 - \gamma_5) \psi_{\nu}, \quad (1)$$

$$J_{\lambda}^{(0)} = \bar{\psi}_N \left\{ F_1^Z \gamma_{\lambda} + F_2^Z \frac{i\sigma_{\lambda\nu} q^{\nu}}{2M_N} + G_A \gamma_{\lambda} \gamma_5 \right\} \psi_N. \quad (2)$$

The neutral weak form factors in the hadronic current account for the fact that protons and neutrons are extended objects. They are constructed from the underlying quark-currents and are given by ( $\tau_3 = \pm 1$  for protons, neutrons):

$$F_{1,2}^Z = \left( \frac{1}{2} - \sin^2 \theta_W \right) \left[ \frac{F_{1,2}^p - F_{1,2}^n}{2} \right] \tau_3 - \sin^2 \theta_W \left[ \frac{F_{1,2}^p + F_{1,2}^n}{2} \right] - \frac{1}{2} F_{1,2}^s, \quad (3)$$

$$G_A = -\frac{1}{2} G_A^3 \tau_3 + \frac{1}{2} G_A^s. \quad (4)$$

Arising from the  $s\bar{s}$ -sea,  $F_{1,2}^s$  and  $G_A^s$  are purely iso-scalar and therefore do not contribute to charged current reactions like  $\nu_e$ -capture or  $\beta$ -decay. These strangeness form factors are, in general, not well known. But  $F_1^s$ , corresponding to the charge form factor, has to vanish at zero momentum transfer  $F_1^s(q^2 = 0) = 0$ , because the nucleon is globally strangeless. In low and medium energy neutrino scattering reactions  $F_1^s$  can be neglected, because only low momentum transfers are involved.

One sensitive method to determine the strange quark axial form factor is to measure the ratio of proton-to-neutron neutrino-induced yield  $R_y$  on an iso-scalar nucleus. This is illustrated by the following *rule of thumb*, which is obtained by neglecting final state interactions and assuming that the axial-vector current gives the dominant contribution to the cross section (for  $N = Z$  nuclei, and the axial form factor is set to  $G_A^3 = 1.25$ ):

$$R_y := \frac{(\nu, \nu' p)}{(\nu, \nu' n)} = \frac{(G_A^p)^2}{(G_A^n)^2} = \frac{(-\frac{1}{2}G_A^3 + \frac{1}{2}G_A^s)^2}{(+\frac{1}{2}G_A^3 + \frac{1}{2}G_A^s)^2} \approx 1 - \frac{16}{5}G_A^s + \dots \quad (5)$$

This approximately linear dependence of  $R_y$  on the strange quark axial form factor  $G_A^s$  is confirmed within a full continuum RPA calculation and has been proposed as a sensitive way to measure  $G_A^s$  at LAMPF [25, 26]. In Fig. 4 we show the results of this calculation obtained with the sum of the  $\bar{\nu}_{\mu}$ - and  $\nu_{\mu}$ -fluxes available at LAMPF. Note, that the ratio of integrated proton-

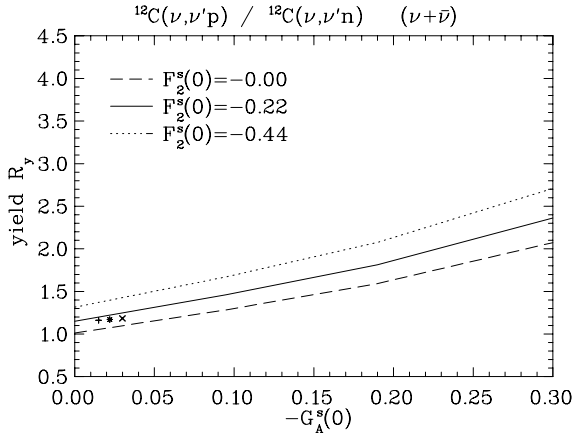


Fig. 4. Ratio of integrated proton-to-neutron yield for quasi-elastic (anti)neutrino reactions on  $^{12}\text{C}$  as a function of  $-G_A^s(0)$  for different values of  $F_2^s(0)$  within the theoretically estimated regime [23, 27]. The symbols indicate the predictions of a SU(3) Skyrme model of the nucleon with vector mesons [28]. Their location on the horizontal axis reflects the associated prediction for  $G_A^s(0)$ .

to-neutron yield also depends on the value of  $F_2^s(0)$ , which does not allow for a unique and precise determination of  $G_A^s(0)$  from a single measurement of  $R_y$ .

Another method to determine the strangeness content of the nucleon, which we just touch here, is to look for neutrino-induced excitation of nuclear levels which are forbidden by selection rules otherwise (so called strangeness-allowed transitions) [29].

### 3.3. Neutrino induced reactions on $^{12}\text{C}$

The (major) physics aim of the KARMEN [7] and LSND [30] experiments is given by the search for neutrino oscillations in the  $\nu_\mu \rightarrow \nu_e$  and  $\bar{\nu}_\mu \rightarrow \bar{\nu}_e$  appearance channels, and their observation of neutrino-nucleus interactions appears more like 'bread and butter' physics. Nevertheless, the extraction of these cross sections is of substantial importance for a number of reasons:

- These measurements provide valuable information about the response of the detector.
- They serve for testing our picture of nuclear structure.
- The agreement between the calculated and experimental result for the  $^{12}\text{C}(\nu, \nu')^{12}\text{C}^*(1^+, 1; 15.11\text{MeV})$ -cross section confirmed the structure of the weak neutral current as given within the Standard Model [31].

- The measured ratio of the neutral to charged current induced cross sections on  $^{12}\text{C}$  corresponded to the value expected from theory, which implied a new test of the  $\nu_e, \bar{\nu}_\mu$  universality [32].
- An analysis of the electron spectrum from the  $^{12}\text{C}(\nu_e, e^-)^{12}\text{N}_{\text{g.s.}}$ -reaction has put stringent upper limits on non-standard contributions to the weak charged current [33,34].

TABLE I

Comparison of measured and calculated exclusive cross sections for charged and neutral current neutrino scattering on  $^{12}\text{C}$  in units of  $10^{-42}\text{cm}^2$ .

Reaction	Theory	Ref.	Exp.	Ref.
$^{12}\text{C}(\nu_e, e^-)^{12}\text{N}_{\text{g.s.}}$	9.4	[35]	$10.5 \pm 1.0(\text{stat.}) \pm 1.0(\text{syst.})$	[39]
	9.2	[36]	$9.1 \pm 0.5(\text{stat.}) \pm 0.8(\text{syst.})$	[32]
	8.9	[37]	$9.1 \pm 0.4(\text{stat.}) \pm 0.9(\text{syst.})$	[40]
	8.0	[38]		
$^{12}\text{C}(\nu_\mu, \mu^-)^{12}\text{N}_{\text{g.s.}}$	68	[37]	$66 \pm 10(\text{stat.}) \pm 10(\text{syst.})$	[41]
$^{12}\text{C}(\nu, \nu')^{12}\text{C}^*(15.1)$	10.5	[37]	$10.4 \pm 1.0(\text{stat.}) \pm 0.9(\text{syst.})$	[32]
$^{12}\text{C}(\nu_\mu, \nu'_\mu)^{12}\text{C}^*(15.1)$	2.8	[37]	$3.2 \pm 0.5(\text{stat.}) \pm 0.4(\text{syst.})$	[42]
$\sigma_{nc}/\sigma_{cc}$	1.18	[37]	$1.15 \pm 0.13(\text{stat.}) \pm 0.06(\text{syst.})$	[32]

TABLE II

The inclusive muon capture rate  $\omega$ , (in  $10^3 \text{ s}^{-1}$ ) and the cross sections for the  $^{12}\text{C}(\nu_e, e^-)^{12}\text{N}^*$  (in units of  $10^{-42} \text{ cm}^2$ ) and the total (inclusive + exclusive) cross section for the  $^{12}\text{C}(\nu_\mu, \mu^-)^{12}\text{N}$  (in  $10^{-40} \text{ cm}^2$ ) reactions in comparison with the data.

Reaction	Theory	Ref.	Exp.	Ref.
$^{12}\text{C}(\mu^-, \nu_\mu)^{12}\text{B}^*$	32.7	[37]	$32.8 \pm 0.8$	[46]
$^{12}\text{C}(\nu_e, e^-)^{12}\text{N}^*$	3.7	[35]	$5.1 \pm 0.6(\text{stat.}) \pm 0.5(\text{syst.})$	[47]
	5.4	[37]	$5.7 \pm 0.6(\text{stat.}) \pm 0.6(\text{syst.})$	[40]
	9.8	[43]		
$^{12}\text{C}(\nu_\mu, \mu^-)\text{X}$	1780	[37]	$1240 \pm 30(\text{stat.}) \pm 180(\text{syst.})$	[48]
	1900	[44]	$1120 \pm 30(\text{stat.}) \pm 180(\text{syst.})$	[41]
	1310	[43]	$830 \pm 70(\text{stat.}) \pm 160(\text{syst.})$	[49]
	1350-1450	[45]		

For most of the neutrino induced reactions the cross sections calculated within different models and the results of various experiments were all found to be in good agreement. Such a consistent picture emerged for all exclusive

transitions, in which the excitation of a specific final state is measured. This nice agreement between theory and experiment is shown in Table I.

However, the situation is somewhat different for the measured and calculated cross sections of inclusive reactions, which are shown in Table II. While the agreement between theory and experiment concerning the muon capture rate on  $^{12}\text{C}$  and the  $^{12}\text{C}(\nu_e, e^-)^{12}\text{N}^*$  cross section is good, there is a clear discrepancy between calculation and measurement for the inclusive  $^{12}\text{C}(\nu_\mu, \mu^-)\text{X}$  cross section. As the measured value for the cross section went up within the last 5 years, this disturbing discrepancy became less severe than before. But it still requires further experimental and theoretical investigations.

### 3.4. Lead and iron in neutrino detectors

Some of the supernova-neutrino or neutrino-oscillation detectors use iron or lead as detector material (*e.g.* MINOS [6], LAND [50] and OMNIS [51]) or have adopted steel (LSND, KARMEN) and lead (LSND) shielding. Thus, precise theoretical estimates of the neutrino-induced cross sections on Fe and Pb are required for a reliable knowledge of the detection signal or the appropriate simulation of background events. We note that the KARMEN collaboration has recently measured the total  $^{56}\text{Fe}(\nu_e, e^-)^{56}\text{Co}$  cross section by using their sensitivity to  $\nu_e$ -induced background events in the iron shielding of the KARMEN detector [52]. In Ref. [53] we have calculated this cross section in a hybrid model in which the allowed transitions have been studied based on the interacting shell model, while the forbidden transitions were calculated within the continuum random phase approximation, and found good agreement with the KARMEN-data. But more detailed theoretical work is necessary, especially partial cross sections for knocking out neutrons by charged- or neutral-current neutrino-induced excitation of  $^{56}\text{Fe}$  and  $^{208}\text{Pb}$  must be determined. We have started such calculations within the hybrid model for  $^{56}\text{Fe}$  and within the RPA model with renormalized Gamow-Teller strength for  $^{208}\text{Pb}$ , and will present first results in the following. Details can be found in an upcoming paper [54].

The distribution of the various supernova neutrino species is usually described by a Fermi-Dirac spectrum

$$n(E_\nu) = \frac{1}{F_2(\alpha)T^3} \frac{E_\nu^2}{\exp[(E_\nu/T) - \alpha] + 1}, \quad (6)$$

where  $T, \alpha$  are parameters fitted to numerical spectra, and  $F_2(\alpha)$  normalizes the spectrum to unit flux. The transport calculations of Janka [55] yield spectra with  $\alpha \sim 3$  for all neutrino species. While this choice also gives good fits to the  $\nu_e$  and  $\bar{\nu}_e$  spectra calculated by Wilson and Mayle [56], their

$\nu_x$  spectra favor  $\alpha = 0$ . Table III summarizes the total and partial cross sections for neutral current reactions on  $^{56}\text{Fe}$  and  $^{208}\text{Pb}$  for both values of  $\alpha$ . In particular we include results for those  $(T, \alpha)$  values which are currently

TABLE III

Total cross sections for neutral current neutrino scattering on nuclei for different neutrino energy spectra represented as Fermi–Dirac distributions. The cross sections are given in units of  $10^{-42}\text{cm}^2$  and are averaged over neutrinos and antineutrinos.

$(T, \alpha)$	(4,0)	(6,0)	(8,0)	(3,3)	(4,3)	(6,3,3)
$^{56}\text{Fe}(\nu, \nu'\gamma)^{56}\text{Fe}$	2.5e 0	9.8e 0	1.7e 1	1.2e 0	4.4e 0	1.6e 1
$^{56}\text{Fe}(\nu, \nu'n)^{55}\text{Fe}$	8.9e-1	6.7e 0	2.2e 1	2.8e-1	1.7e 0	1.4e 1
$^{56}\text{Fe}(\nu, \nu'p)^{55}\text{Mn}$	1.2e-1	1.0e 0	3.6e 0	3.4e-2	2.3e-1	2.2e 0
$^{56}\text{Fe}(\nu, \nu'\alpha)^{52}\text{Cr}$	2.4e-2	1.9e-1	6.6e-1	6.4e-3	4.4e-2	4.0e-1
$^{56}\text{Fe}(\nu, \nu')\text{X}$	3.6e 0	1.8e 1	4.3e 1	1.5e 0	6.3e 0	3.3e 1
$^{208}\text{Pb}(\nu, \nu'\gamma)^{208}\text{Pb}$	1.4e 0	7.4e 0	2.1e 1	7.0e-1	2.5e 0	1.5e 1
$^{208}\text{Pb}(\nu, \nu'n)^{207}\text{Pb}$	1.2e 1	4.8e 1	1.2e 2	6.9e 0	2.0e 1	9.4e 1
$^{208}\text{Pb}(\nu, \nu'p)^{207}\text{Tl}$	1.6e-5	3.5e-4	2.4e-3	2.9e-6	3.1e-5	9.0e-4
$^{208}\text{Pb}(\nu, \nu'\alpha)^{204}\text{Hg}$	7.8e-5	3.0e-3	2.6e-2	8.1e-6	1.5e-4	7.9e-3
$^{208}\text{Pb}(\nu, \nu')\text{X}$	1.3e 1	5.6e 1	1.4e 2	7.6e 0	2.3e 1	1.1e 2

avored for the various neutrino types ( $T$  in MeV):  $(T, \alpha) = (4,0)$  and  $(3,3)$  for  $\nu_e$  neutrinos,  $(5,0)$  and  $(4,3)$  for  $\bar{\nu}_e$  neutrinos and  $(8,0)$  and  $(6,3,3)$  for  $\nu_x$  neutrinos.

For  $^{56}\text{Fe}$  the neutron and proton thresholds open at 11.2 MeV and 10.18 MeV, respectively. But despite the slightly higher threshold energy, the additional Coulomb barrier in the proton channel makes the neutron channel the dominating decay mode. Also for  $^{208}\text{Pb}$  most of the neutral current neutrino scattering events lead to the emission of a neutron, and partial and total cross sections grow significantly with increasing neutrino energy.

One of the goals in building supernova-neutrino detectors with lead and iron is to distinguish  $\nu_x$  neutrinos from  $\nu_e$  and  $\bar{\nu}_e$  (anti)neutrinos by counting the number of knocked-out neutrons. Whereas  $\nu_\mu$  and  $\nu_\tau$  neutrinos, due to their higher energies, were expected to excite high lying states in the nucleus which decay via emission of several neutrinos, low energy  $\nu_e$  and  $\bar{\nu}_e$  (anti)neutrinos should just be able to knock-out one nucleon at most. The huge total and partial cross sections for charged current ( $\nu_e, e^-$ ) reactions on  $^{56}\text{Fe}$  and  $^{208}\text{Pb}$  listed in Table IV show that this method of discriminating neutrinos of different flavor is very problematic. The differences in the ratios for neutral and charged current neutron yields exemplify the more general

TABLE IV

Total cross sections for charged current neutrino scattering on nuclei for different neutrino energy spectra represented as Fermi–Dirac distributions. The cross sections are given in units of  $10^{-42}\text{cm}^2$ .

$(T, \alpha)$	(4,0)	(6,0)	(8,0)	(3,3)	(4,3)	(6,3,3)
$^{56}\text{Fe}(\nu_e, e^- \gamma)^{56}\text{Co}$	9.8e 0	3.1e 1	6.1e 1	7.7e 0	2.1e 1	7.5e 1
$^{56}\text{Fe}(\nu_e, e^- n)^{55}\text{Co}$	7.5e-1	8.0e 0	3.2e 1	2.5e-1	1.7e 0	2.0e 1
$^{56}\text{Fe}(\nu_e, e^- p)^{55}\text{Fe}$	5.4e 0	3.2e 1	9.7e 1	9.2e-1	5.1e 0	4.7e 1
$^{56}\text{Fe}(\nu_e, e^- \alpha)^{52}\text{Mn}$	6.1e-2	9.7e-1	4.8e 0	3.0e-2	2.1e-1	2.9e 0
$^{56}\text{Fe}(\nu_e, e^-)X$	1.6e 1	7.2e 1	1.9e 2	8.9e 0	2.8e 1	1.4e 2
$^{208}\text{Pb}(\nu_e, e^- \gamma)^{208}\text{Bi}$	7.3e 1	2.6e 2	5.8e 2	4.9e 1	1.2e 2	4.8e 2
$^{208}\text{Pb}(\nu_e, e^- n)^{207}\text{Bi}$	3.0e 2	1.5e 3	3.7e 3	1.5e 2	5.5e 2	2.9e 3
$^{208}\text{Pb}(\nu_e, e^- p)^{207}\text{Pb}$	2.5e-2	1.9e-1	6.5e-1	9.2e-3	4.7e-2	4.2e-1
$^{208}\text{Pb}(\nu_e, e^- \alpha)^{204}\text{Tl}$	2.5e-2	3.2e-1	1.5e 0	5.3e-3	4.7e-2	7.6e-1
$^{208}\text{Pb}(\nu_e, e^-)X$	3.8e 2	1.7e 3	4.3e 3	2.0e 2	6.7e 2	3.4e 3

tendency that neutral-current cross sections for supernova  $\nu_x$  neutrinos scale approximately with the mass number  $A$  of the target, while the charged-current cross sections for supernova  $\nu_e$  neutrinos depends on the  $N - Z$  neutron excess of the target via the Fermi and Ikeda sumrules (*e.g.* [57]). This suggests [58] that neutrino detectors which can only determine total neutron counting rates can have supernova neutrino spectroscopy ability, if they are made of various materials with quite different  $Z$  values as the ratio of neutral- to charged-current cross sections is quite sensitive to the charge number of the detector material.

Both the LAND and the OMNIS detectors will also be capable of detecting the neutron energy spectrum following the decay of states in the daughter nucleus after excitation by charged- and neutral-current neutrino reactions. We have calculated the relevant neutron energy spectra for both possible detector materials,  $^{56}\text{Fe}$  and  $^{208}\text{Pb}$ . To this end we have used the statistical model code SMOKER iteratively by following the decay of the daughter states after the first particle decay. We have kept book of the neutron energies produced in these (sequential) decays and have binned them in 500 keV bins. The energy spectrum of neutrons from charged current reactions on  $^{208}\text{Pb}$  is shown in Fig. 5. Note that the relative height of the peak at  $E_n = 1.25$  MeV sitting on a broader hump is more pronounced for the  $(T, \alpha) = (4, 0)$  neutrino distribution than for a potential  $(T, \alpha) = (8, 0)$   $\nu_e$  spectrum as it might arise after complete  $\nu_\mu \leftrightarrow \nu_e$  oscillations. Whereas the peak is due to one-neutron decay of lower excited  $1^+$ -states in  $^{208}\text{Pb}$ , the hump is caused by 2-neutron decay of higher excited resonances, in which

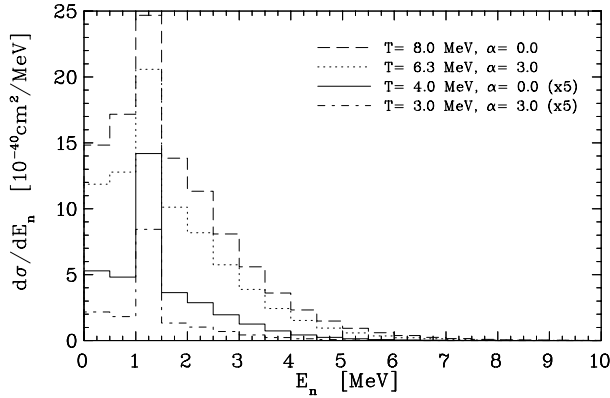


Fig. 5. Neutron energy spectrum produced by the charged-current ( $\nu_e, e^-$ ) reaction on  $^{208}\text{Pb}$ . The calculation has been performed for different supernova neutrino spectra characterized by the parameters  $(T, \alpha)$ . Note that the cross sections for  $(T, \alpha) = (4, 0)$  and  $(3, 3)$  neutrinos have been scaled by a factor 5.

case the available energy is shared between the two emitted particles. Therefore a corresponding shape analysis of neutron energy spectra could help in the search for  $\nu_x \rightarrow \nu_e$  oscillations.

#### 4. Conclusions

By means of a selection of applications we have tried to emphasize the important role of neutrino induced reactions on nuclei at low and intermediate energies both in accelerator-based experiments and in Neutrino Astrophysics. In detail we found that:

- photons with energies between 5 – 10 MeV, generated by  $(\nu, \nu' p \gamma)$  and  $(\nu, \nu' n \gamma)$  reactions on  $^{16}\text{O}$ , constitute a signal for supernova  $\mu$  and  $\tau$  neutrinos,
- the ratio  $^{12}\text{C}(\nu, \nu' p)/^{12}\text{C}(\nu, \nu' n)$  depends on the strangeness content of the nucleon,
- the discrepancy between theory and experiment for the  $^{12}\text{C}(\nu_\mu, \mu^-)X$  cross section remains a serious problem,
- we can provide good theoretical estimates of neutrino scattering cross sections, branching ratios and the energy spectra of emitted nucleons, which are needed for experiments in Neutrino Physics and Nuclear Astrophysics.

Finally we just mention here that neutrino induced transmutation of nuclei will also play an important role in (at least) two acts of a Type II supernova spectacle. In the hot, neutron-rich bubble, an intense neutrino flux could affect the outcome of the r-process by spallation of neutron-rich nuclei after the freeze-out [57]. And by scattering on the (heavy) elements in the overlying shells of the pre-supernova star, a significant amount of rare isotopes can be produced (so called neutrino-nucleosynthesis). Such calculations are in progress.

This work was supported by the Swiss National Science Foundation.

## REFERENCES

- [1] G. Raffelt, *Stars as Laboratories for Fundamental Physics*, Chicago Press, 1996.
- [2] C. Athanassopoulos *et al.* (LSND Collaboration), *Phys. Rev. Lett.* **75**, 3082 (1995); *Phys. Rev. Lett.* **81**, 1774 (1998).
- [3] J.N. Bahcall, *Neutrino Astrophysics*, Cambridge University Press, 1989.
- [4] Y. Fukuda *et al.*, *Phys. Rev. Lett.* **81**, 1562 (1998).
- [5] T. Stanev, *Nucl. Phys.* **B48**, 165 (1996).
- [6] P. Adamson *et al.*, MINOS collaboration, The MINOS Detectors Technical Design Report, NuMI-L-337 (October 1998).
- [7] G. Drexlin *et al.*, KARMEN Collaboration, in *Proceedings of Neutrino Workshop, Heidelberg 1987*, eds B. Povh and V. Klapdor, Springer Verlag, 1987, p. 147.
- [8] B. Armbruster *et al.* (KARMEN Collaboration), *Phys. Rev.* **C57**, 3414 (1998) and references therein.
- [9] E. Kolbe, K. Langanke, S. Krewald, F.-K. Thielemann, *Nucl. Phys.* **A540**, 599 (1992).
- [10] K. Nakayama, S. Drożdż, S. Krewald, J. Speth, *Nucl. Phys.* **A470**, 573 (1987).
- [11] R. Machleidt, K. Holinde, Ch. Elster, *Phys. Rep.* **149**, 1 (1987).
- [12] S. Krewald, K. Nakayama, J. Speth, *Phys. Rep.* **161**, 103 (1988).
- [13] J.J. Cowan, F.-K. Thielemann, J.W. Truran, *Phys. Rep.* **208**, 267 (1991).
- [14] E. Kolbe, thesis, Universität Münster (1992).
- [15] M. Buballa, S. Drożdż, S. Krewald, J. Speth, *Ann. Phys.* **208**, 346 (1991).
- [16] B. Zeitnitz *et al.*, KARMEN Collaboration, *Prog. Part. Nucl. Phys.* **32**, 351 (1994).
- [17] E. Kolbe, K. Langanke, P. Vogel, *Phys. Rev.* **C50**, 2576 (1994).
- [18] Y. Totsuka, *Rep. Progr. Phys.* **55**, 377 (1992).

- [19] F. Ajzenberg-Selove, *Nucl. Phys.* **A523**, 1 (1991).
- [20] K. Langanke, P. Vogel, E. Kolbe, *Phys. Rev. Lett.* **76**, 2629 (1996).
- [21] J. Ashman *et al.*, (EMC Collaboration), *Nucl. Phys.* **B328**, 1 (1989).
- [22] L.A. Ahrens *et al.*, *Phys. Rev.* **D35**, 785 (1987).
- [23] R.L. Jaffe, A. Manohar, *Nucl. Phys.* **B337**, 509 (1990).
- [24] M.J. Musolf, T.W. Donnelly, J. Dubach, S.J. Pollock, S. Kowalski, E.J. Beise, *Phys. Rep.* **239**, 1 (1994).
- [25] G.T. Garvey, S. Krewald, E. Kolbe, K. Langanke, *Phys. Lett.* **B289**, 249 (1992).
- [26] G.T. Garvey, E. Kolbe, K. Langanke, S. Krewald, *Phys. Rev.* **C48**, 1919 (1993).
- [27] R.L. Jaffe, *Phys. Lett.* **B229**, 275 (1989).
- [28] E. Kolbe, S. Krewald, H. Weigel, *Z. Phys.* **A358**, 445 (1997).
- [29] E. Kolbe, K. Langanke, S. Krewald, F.-K.Thielemann, *Astrophys. J. Lett.* **401**, L89 (1992).
- [30] W.C. Louis, LAMFP Research Report No. LA-UR-89-3764 (1989).
- [31] B. Bodmann *et al.*, KARMEN Collaboration, *Phys. Lett.* **B267**, 321 (1991).
- [32] B.E. Bodmann *et al.*, KARMEN Collaboration, *Phys. Lett.* **B332**, 251 (1994).
- [33] W. Fetscher, *Phys. Rev. Lett.* **71**, 2511 (1993).
- [34] G. Drexlin *et al.*, KARMEN Collaboration, *Prog. Part. Nucl. Phys.* **32**, 375 (1994) and references therein.
- [35] T.W. Donnelly, *Phys. Lett.* **B43**, 93 (1973).
- [36] M. Fukugita, Y. Kohyama, K. Kubodera, *Phys. Lett.* **B212**, 139 (1988).
- [37] E. Kolbe, K. Langanke, P. Vogel, *Nucl. Phys.* **A652**, 91 (1999).
- [38] S.L. Mintz, M. Pourkaviani, *Nucl. Phys.* **A594**, 346 (1995).
- [39] R.C. Allen, H.H. Chen, P.J. Doe, R. Hausmann, W.P. Lee, *Phys. Rev. Lett.* **64**, 1871 (1990).
- [40] C. Athanassopoulos *et al.*, LSND Collaboration, *Phys. Rev.* **C55**, 2078 (1997).
- [41] C. Athanassopoulos *et al.*, LSND Collaboration, *Phys. Rev.* **C56**, 2806 (1997).
- [42] B. Armbruster *et al.*, KARMEN Collaboration, *Phys. Lett.* **B423**, 15 (1998).
- [43] S.L. Mintz, M. Pourkaviani, *Nucl. Phys.* **A594**, 346 (1995).
- [44] T.S. Kosmas, E. Oset, *Phys. Rev.* **C53**, 1409 (1996).
- [45] N. Auerbach *et al.*, *Phys. Rev.* **C56**, 2368 (1997).
- [46] T. Suzuki *et al.*, *Phys. Rev.* **C35**, 2212 (1987).
- [47] J. Kleinfeller *et al.*, KARMEN Collaboration, *Neutrino '96*.
- [48] R. Imlay, private communication (1998).
- [49] M. Albert *et al.*, *Phys. Rev.* **C51**, 1065 (1995).

- [50] C.K. Hargrove *et al.*, *Astropart. Phys.* **5**, 183 (1996).
- [51] P.F. Smith, *Astropart. Phys.* **8**, 27 (1997).
- [52] R. Maschuw, *Prog. Part. Nucl. Phys.* **40**, 183 (1998).
- [53] E. Kolbe, K. Langanke and G. Martínez-Pinedo, *Phys. Rev.* **C60**, 052801-1 (1999).
- [54] E. Kolbe, K. Langanke, *The Role of  $\nu$ -Induced Reactions on Lead and Iron in Neutrino Detectors*, submitted to *Phys. Rev. C* (March, 2000).
- [55] H.-T. Janka, W. Hillebrandt, *Astron. Astrophys.* **224** 49 (1989); *Astron. Astrophys. Suppl.* **78** 375 (1989).
- [56] J.R. Wilson, private communication.
- [57] A. Hektor, E. Kolbe, K. Langanke, J. Toivanen, *Phys. Rev.* **C61**, 055803-1 (2000).
- [58] G.M. Fuller, W.C. Haxton, G.C. McLaughlin, *Phys. Rev.* **D59**, 085005 (1999).